

## Experiments on the hot-tool welding of three dissimilar thermoplastics\*

Vijay K. Stokes

*GE Corporate Research and Development, Schenectady, NY 12301, USA*

*(Received 9 January 1997)*

A dual platen hot-tool welding machine, in which the temperatures of the two hot-tool surfaces can be independently controlled, is used to study the weldability of the three dissimilar thermoplastics—polycarbonate, polyetherimide, and poly(butylene terephthalate) to each other. In these experiments, the outflow in the melting phase is controlled by means of stops, the thickness of the molten film is controlled by the heating time, and the outflow during the final joining phase is also controlled by displacement stops. Strength data for butt welds are reported for a series of tests in which the hot-tool surface temperatures and the melt (heating) times were varied, but the displacement stop positions and the weld pressure were not. High weld strengths are demonstrated for each pair from these three dissimilar thermoplastics. © 1998 Elsevier Science Ltd. All rights reserved.

**(Keywords: hot-tool welding; dissimilar materials; polycarbonate)**

### INTRODUCTION

Because of the increasing use of thermoplastics and thermoplastic composites in load-bearing applications, welding methods are becoming important for part cost reduction. Welding requires the melting of the surfaces to be joined, followed by a solidification of the interfacial molten layers under pressure. One widely used technique is hot-tool welding, in which the surfaces to be joined are brought to the 'melting temperature' by direct contact with a heated metallic tool. In some cases, such as in joining of plastic pipes, the surfaces to be joined are flat, so that the tool is a hot plate. However, in many applications, such as in automotive head lamps and rear lights, doubly-curved joint interfaces require complex tools that allow the hot surfaces to match the contours of the joint interface. Applicability to complex geometries is one of the major advantages of this process. This technique can also be used for welding dissimilar materials, which is becoming important for reducing part cost by multimaterial use. Only critical components of a part need be made of expensive plastic; these components can then be welded to the rest of the part made from inexpensive plastic. For example, an automotive head lamp assembly is made by welding a clear polycarbonate lens to an inexpensive plastic body. In some high-temperature applications, a fascia made of a relatively more expensive high-temperature plastic can be welded to a less expensive subcomponent. This paper examines the hot-tool weldability of three dissimilar engineering thermoplastics: the two amorphous resins polycarbonate and polyetherimide, and the semicrystalline resin poly(butylene terephthalate).

The hot-tool welding process can be described in terms of the four phases schematically shown by the pressure-time diagram in *Figure 1*<sup>1</sup>. In phase 1, the parts are brought into

contact with the hot-tool, and a relatively high pressure is used to ensure complete matching of the part and tool surfaces. The pressure is maintained until the molten plastic begins to flow out laterally. In phase 2, the melt pressure is reduced to allow the molten film to thicken. The rate at which the film thickens is controlled by heat conduction through the molten layer. When a sufficient film thickness has been achieved, the part and tool are separated. This third phase is referred to as the changeover phase; its duration should be kept to a minimum to prevent premature cooling of the molten film. The molten interfaces of the parts to be joined are then brought together and held under pressure until the weld solidifies. During this final joining phase the molten material flows laterally outward, while undergoing cooling and solidification. Clearly, the important welding parameters for this process are the hot-tool temperature during phases 1 and 2, the matching pressure during phase 1, the melt pressure during phase 2, the changeover time and the separation and rejoining velocities, and the weld pressure and duration of phase 4. This hot-tool welding technique—commonly referred to as welding by pressure—requires machines in which the applied pressure can be accurately controlled. One shortcoming of this process is that the final part dimensions are not controlled directly. In particular, variations in the part-to-part film thickness and the sensitivity of the melt viscosities of thermoplastics to small temperature changes can result in unacceptable variations in part dimensions.

A modification of the above method, called welding by distance, uses rigid stops to control the process and part dimensions. As in welding by pressure, the parts to be joined are first forced against the hot-tool, but the displacements of the parts during phase 1 are restricted to a predetermined distance by means of mechanical stops. In phase 2, the parts are held in place against the stops for a predetermined time to allow the molten layer to thicken. During the final joining phase, mechanical stops are again used to inhibit the motion of the parts, thereby allowing the molten film to solidify solely by heat conduction, without any gross flow. In this

\*Based on a paper presented at the Society of Plastics Engineers 51st Annual Technical Conference, 9-13 May 1993, New Orleans, Louisiana, USA

way part dimensions can be controlled more accurately. However, computer controlled machines, in which pressure or displacement can be programmed over different phases of the welding cycle, are now available<sup>2</sup>.

Although considerable progress has been made in experimentally characterizing hot-tool welding<sup>3-11</sup> the underlying process physics has been analyzed in terms of highly simplified models<sup>2,12-15</sup>. For example, these models assume that the melt viscosity is constant during the final joining phase. Any realistic model for the welding process<sup>16</sup> must account for the fact that the viscosity of polymer melts can decrease by more than factor of two for a 10°C increase in temperature. A more recent analysis of the hot-tool welding process<sup>17</sup> has shown that this temperature

sensitivity has a dramatic effect on the process conditions within the molten layer. That analysis has also shown how the use of stops affects the welding process.

In principle, any polymer that melts on heating can be welded by the hot-tool welding process. By using different hot-tool temperatures for the two halves of an assembly, it should be possible to weld dissimilar materials<sup>18,19</sup>. The literature on the welding of dissimilar materials is quite small. The few papers on hot-tool welding are mainly concerned with the weldability of different grades of HDPE<sup>20,21</sup> and the welding of PP homopolymer to a PP copolymer<sup>22</sup>. Certainly, this topic has not been explored systematically. Also, process models have not been developed for the welding of dissimilar materials. Recent studies on the vibration welding of dissimilar materials have shown that it is possible to obtain high strengths between welds of bisphenol-A polycarbonate (PC) and polyetherimide (PEI)<sup>23</sup>, and between PC and poly(butylene terephthalate) (PBT)<sup>24</sup>. The strengths of vibration welds of ABS to PC, PBT, PEI, and modified polyphenylene oxide are explored in Ref. 25. This paper examines that hot-tool welding of PC, PBT, and PEI to each other.

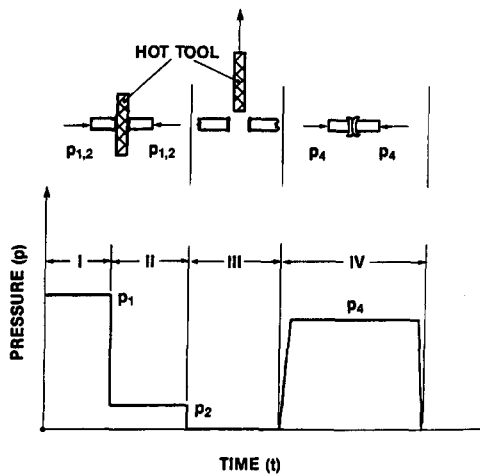


Figure 1 Schematic pressure-time graph showing the four phases of the hot-tool welding process (adapted from Ref. 2)

#### DISPLACEMENT CONTROLLED WELDING

The essential parts of a hot-tool welding machine consist of the hot-tool assembly having two exposed hot surfaces, two fixtures for holding the parts to be welded, means for bringing the parts into contact with hot surfaces and then bringing the molten surfaces together to form the weld, together with adequate timing and displacement controls. The mechanics of the hot-tool welding process using mechanical stops to effect displacement control can be

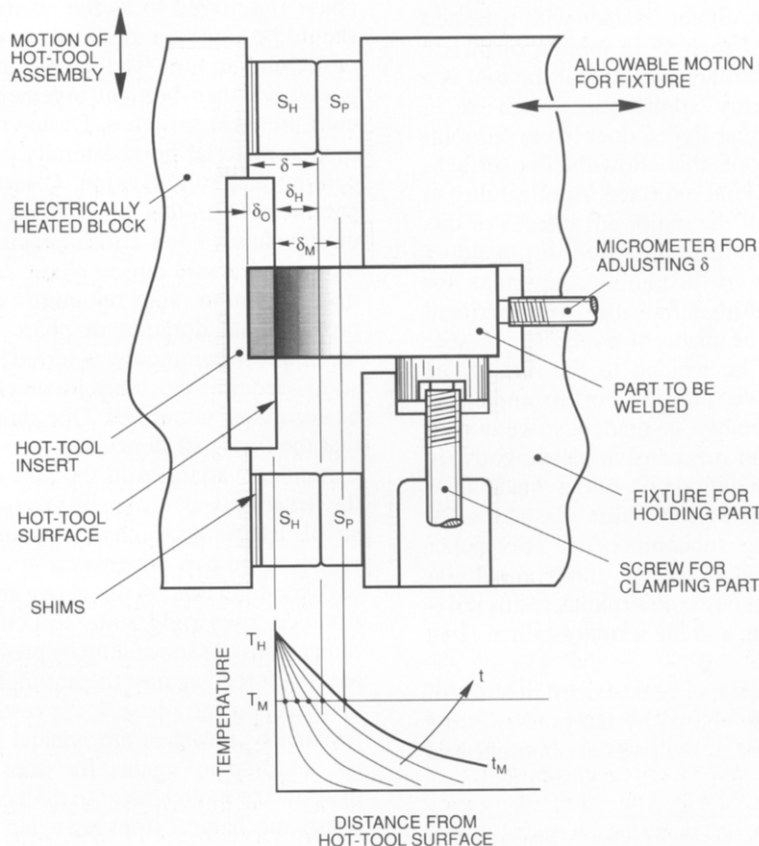


Figure 2 Schematic diagram showing geometric parameters for displacement-controlled hot-tool welding using mechanical stops

described by means of the schematic in *Figure 2*. The left-hand side of this figure shows one half of the hot-tool assembly, comprising an electrically heated block on which interchangeable hot-tool inserts (in this case a flat insert) can be mounted. Normally, a single hot-tool that has two exposed hot surfaces is used for heating the two halves of an assembly, especially for flat-surfaced parts made of the same material. However, in dual platen hot-tool machines the two halves can be independently heated to maintain the two exposed surfaces at different temperatures—this capability is essential for welding dissimilar materials having different ‘melt’ temperatures. The hot-tool assembly has mechanical stops  $S_H$  whose surfaces are offset from the hot-tool surface by a distance  $\delta_H$ . The hot-tool assembly can be moved in and out of the configuration shown in the figure along the direction indicated.

The part to be welded is gripped in a fixture (right-hand side of the figure), that can be moved to and fro in a direction at right angles to the allowable motion for the hot-tool assembly. This fixture has mechanical stops  $S_P$  that are aligned with the hot-tool stops  $S_H$ . Let the distance by which the parts surface protrudes beyond the surfaces of the stops  $S_P$  be  $\delta = \delta_0 + \delta_H$ , as shown in the figure.

For welding, the hot-tool assembly is first moved into the position shown. Then the part fixture is moved in the direction indicated to bring it into contact with the hot-tool surface, and a pressure is applied to maintain this contact. (Clearly, contact is possible only when  $\delta \geq \delta_H$ .) The part surface heats up and begins to melt. The externally applied pressure causes the molten material to flow laterally outward, thereby inducing a leftward motion of the part. The decrease in the part length caused by the outflow of molten material will be called the penetration  $\eta$ , which for this phase will be the part displacement from the instant of contact, and weld time will be measured from this instant. Initially, when the surface begins to melt, there will be very little flow—and therefore the penetration will be very small—and the molten film will thicken. The flow and penetration rate will begin to increase with time, eventually resulting in a steady state in which the outflow rate will equal the rate at which the material is melting; from this point on the penetration will increase linearly with time<sup>16</sup>. However, when stops are used, the penetration (or part motion) will cease when the part stops  $S_P$  come into contact with the hot-tool stops  $S_H$ , as shown in *Figure 2*<sup>17</sup>. (Of course, stop contact can occur before the steady-state is attained.) Let the elapsed time from the instant that the part touches the hot-tool surface to the instant when the stops come into contact be  $t_0$ , and let the corresponding penetration by  $\eta = \delta_0$  (*Figure 2*). Clearly this thickness of the material will flow out laterally to form a part of the weld ‘bead’. After time  $t_0$ , continuing contact with the hot-tool surface will cause the molten layer to thicken with time. The melt/solid interface can be defined as the surface in the material that has attained the ‘melting’ temperature  $T_M$ . During this phase there will be no additional penetration. Let the duration of this film buildup phase be  $t_M$  and let the molten layer thickness be  $\delta_M$  as shown. In the changeover phase, the parts are pulled away from the hot-tool, the hot-tool is retracted, and the molten surfaces are brought into contact—thereby initiating the joining phase. Let the duration of this changeover phase be  $t_c$ . After the molten surfaces touch, the applied joining pressure squeezes out the molten material laterally, resulting in a further penetration. During this squeezing motion, heat transfer from the melt results in a cooling and in an

eventual solidification of the melt. To understand the mechanics of welding, the case in which the two halves to be welded are of the same material will first be discussed. The analysis will then be extended to the case of dissimilar materials.

#### Same materials

Two possible cases are important. If  $\delta_M < \delta_H$ , the part stops  $S_P$  cannot come into contact, so that part dimensions cannot be controlled. But if  $\delta_M > \delta_H$ , the material in the molten material will continue to be squeezed out until the stops  $S_P$  come into contact, after which part motion will stop and the melt will solidify in the absence of further motion. Of course, even when  $\delta_M > \delta_H$ , the stops may not contact if the imposed joining penetration rate is artificially low, so that the material freezes before the stops contact, this case is not of practical importance because the joining penetration rate is high. Thus, for dimensional control  $t_M$  should be large enough to ensure that  $\delta_M > \delta_H$ . For this case, the total penetration on each of the parts being welded will be  $\delta = \delta_0 + \delta_H$  so that the overall part length will decrease by  $2\delta$ , if thermal expansion effects are neglected. Clearly, the melt penetration  $\delta_0$  by itself does not contribute to the welding process during the joining phase; this material just flows outward into the bead. A minimum value of  $\delta_0$  is required to compensate for part surface irregularities and to ensure that contaminated surface layers flow out before the joining phase. The penetration  $\eta_j = \delta_H$  during the joining phase is controlled by the machine setting  $\delta_H$  (*Figure 2*). Let the duration of the joining (or welding) phase, from the instant the molten surfaces touch to the instant the solidified weld is release, be  $t_w$ . Then the total welding time is given by  $t_T = t_0 + t_M + t_c + t_w$ . Clearly,  $t_c$  should be as small as possible.

#### Dissimilar materials

Because of different ‘melt’ temperatures of dissimilar materials and differences in the magnitudes and temperature dependence of their viscosities, the magnitudes of  $\delta_0$  and  $\delta_M$  could be different for the two parts—say,  $\delta_{10}$  and  $\delta_{1M}$ , and  $\delta_{20}$  and  $\delta_{2M}$  for the left and right halves, respectively. Also, because of differences between the viscosities of the two molten layers, the outflows during the joining phase will be different. Again, for dimensional control,  $t_M$  should be large enough to ensure that  $\delta_M > \delta_H$  for each part half. While the total penetration during the joining phase will be  $\delta_{1H} + \delta_{2H}$ —so that the overall part length will decrease by  $\delta_{1H} + \delta_{2H}$ —it will not necessarily result from outflows  $\delta_{1H}$  and  $\delta_{2H}$  from the two halves; rather, the film with the lower viscosity will undergo a larger penetration. Let the initial lengths of the parts before welding be  $l_1$  and  $l_2$ , and let the length of the welded part be  $l_0$ . Then,  $\Delta l = l_1 + l_2 - l_0$  is the thickness of the material that flowed out into the weld bead. If the stops come into contact during the joining phase (for which  $\delta_M > \delta_H$  for each part half) and if thermal expansion effects are neglected, then the expected change in length should be  $\delta_{1H} + \delta_{2H}$ . However, if  $\delta_M < \delta_H$ , then the stops will not come into contact and the change in length should be less than  $\delta_{1H} + \delta_{2H}$ . Thus, if thermal expansion effects are neglected,  $\Delta\eta = \delta_{1H} + \delta_{2H} - \Delta l$  is a measure for whether or not the stops come into contact: stops do and do not contact when  $\Delta\eta = 0$  and  $\Delta\eta > 0$ , respectively. Thermal expansion at the heated ends of the specimens would increase  $\Delta l$  and, in the case in which the stops contact, could result in negative values of the differential penetration  $\Delta\eta$ .

The welding of dissimilar materials therefore requires

dual platen machines in which different hot-tool temperatures can be used for the two materials. Also, an optimization of weld strength may call for different settings  $\delta_{10}$ ,  $\delta_{1M}$  and  $\delta_{20}$ ,  $\delta_{2M}$  for the two materials. While both  $t_0$  and  $t_M$  could also be different for the two part halves, different values of  $t_0$  and  $t_M$  on two sides of the machine would require additional controls to synchronize the changeover and joining phases. For different values of  $t_0 + t_M$  the parts being joined would have to contact their respective hot-tool surfaces at different times, such that changeover and joining are initiated at the same instant. Instead of requiring additional controls, both the part halves could undergo the same time cycles, but with different hot-tool temperatures and different  $\delta_0$  and  $\delta_H$  settings. Note that the 'same' time cycle for the two sides implies that  $t_0 + t_M$  will be the same, but neither  $t_0$  nor  $\delta_M$  need be the same on the two sides.

Thus, from the standpoint of processing, the welding of dissimilar materials involves many more variables than for single materials. In the absence of process models, near optimal conditions must first be established by trying out a matrix of different process conditions. Clearly, the initial choice of process parameters for parts made of two dissimilar materials would be the respective optimal conditions for each of the two materials.

#### TEST PROCEDURE

All of the test data in this paper were obtained from specimens cut from 5.8 mm thick PC extruded sheet material (LEXAN® 9030) and from 6.35 mm thick injection molded plaques of PBT (VALOX® 325) and PEI (ULTEM® 1000). The edges of each specimen were machined to obtain rectangular blocks of size 76.2 × 25.4 mm × thickness for assuring accurate alignment of the surfaces during butt welding along the 25.4 mm × thickness edges.

All of the welds were made on a commercially available (Hydra-Sealer Model VA-1015, Forward Technology Industries, Inc.) dual platen hot-tool welding machine, in which the temperatures of the two hot-tool surfaces can be independently controlled. On this machine, the offset  $\delta_H$  of the hot-tool stop  $S_H$  from the hot-tool surface (Figure 2) can only be changed by inserting shims between the electrically heated hot-tool block and the stops, which are fastened to the block surface by means of screws. Different values of  $\delta_H$  can be set on the two faces of the hot-tool. The weld specimens are pneumatically gripped in special fixtures that accurately align the specimens during the welding cycle. Each grip is provided with a micrometer that can be used to accurately set the distance  $\delta$  by which each specimen protrudes beyond the stops  $S_p$ , any variations in the lengths of the specimens can easily be compensated for. In this machine, the times  $t_0$  and  $t_M$  cannot be resolved, only the total heating time  $t_H = t_0 + t_M$  can be set and measured. However, for  $\delta_0 < \delta_H$ ,  $t_0$  should be much smaller than  $t_M$ . The changeover time  $t_c$ , from the instant the heated specimens are pulled back from the hot-tool to the instant the molten films are brought back into contact, can be changed by changing the decelerating springs and the air pressure on the displacement pistons. However, the possible range of variation is quite small. The welding (joining) time  $t_w$ , measured from the instant the molten films are brought into contact to the instant the (solidified) welded parts are released, can be preset for each weld.

One major shortcoming of this machine is the lack of adequate pressure control at the weld interface. The specimens are loaded by air pressure acting on pistons

that are used to generate the to and fro joining motion. Pressure times the piston cross-sectional area determines the axial load on the specimen, from which the interfacial weld pressure can be calculated. However, near the end of piston travel—when the specimens are about to contact the hot-tool surfaces or when the molten surfaces of the specimens are about to contact during the joining phase—decelerating springs come into play to cushion the contact. As a result, the interfacial pressure during the initial part of the joining phase varies in a way that is a characteristic of the machine. While this variation is repeatable, it has not been characterized for this machine. The nominal weld pressure (based on the air pressure and the piston cross-sectional area) was 3.9 MPa for welds with PC (specimen cross section of 5.8 × 25.4 mm) and 3.5 MPa for welds of PBT to PEI (specimen cross sections of 6.35 × 25.4 mm).

The test procedure is as follows: first, the hot-tool surfaces are allowed to attain the desired surface temperatures. After accurately measuring their lengths, the weld specimens are mounted on the specimen holding fixtures and the micrometer settings are adjusted to obtain desired values of the overhang  $\delta$ . The heating time  $t_H$  and the welding time  $t_w$  are set and the machine is cycled to effect the weld. The weld results in a bar with nominal dimensions of 152.4 × 25.4 mm × thickness. After sufficient cooling, the length of the bar is accurately measured; a difference from the sums of the lengths of the specimens gives  $\Delta l$ . The rectangular bar is then routed down to a standard ASTM D638 tensile test specimen with a butt joint at its center. The tensile bar with a transverse butt weld at mid length is then subjected to a constant displacement rate tensile test in which the strain across the weld is monitored with an extensometer. In this way the average failure strain across the weld over a 25.4 mm gauge length can be monitored. All of the weld strength tensile tests reported in this paper were done at a nominal strain rate of 0.01 s<sup>-1</sup>.

The weld flash or 'bead' was not removed, and the weld strengths were obtained by dividing the load at failure by the original cross-sectional area of the specimen. Because of large local deformations, the true failure stress could be larger than the nominal stress reported in this paper<sup>26</sup>.

Furthermore, the 25.4 mm gauge-length extensometer can grossly underestimate the local strain in the failure region once strain localization sets in, so that the significance of the reported failure strains  $\epsilon_0$  should be interpreted with care. These values only represent the lower limit of the failure strain at the weld.

The slight mismatches in the thickness of the specimens could affect the strengths of the joints of PC to PBT and PEI. But the consequent stress concentration caused by this mismatch would make the strength data in this paper conservative. Strengths are based on the cross-sectional area of the thinner of the two specimens welded.

#### WELD STRENGTH

The main objective of this study was to determine how well PC, PBT, and PEI hot-tool weld to each other, and the optimum welding conditions. This requires experiments over a range of process conditions based on optimum process conditions for the individual materials in a dissimilar pair. Prior to determining the true optimum conditions, an empirical search must first be conducted to find the near optimum conditions for each pair of materials.

The preliminary results in this paper were obtained at a fixed nominal machine setting of  $\delta_H = 0.56$  mm on both

surfaces of the hot-tool. The micrometer settings that control  $\delta_0$ , were set such that a 76.2 mm long specimen would result in a  $\delta_0 = 0.13$  mm. These settings were not adjusted to account for the slight differences ( $\pm 0.08$  mm) in the lengths of the machined specimens. As a result, the actual values of  $\delta_0$  were in the range of 0.05–0.21 mm. The hot-tool temperatures of the two platens were varied, as was the heating time  $t_0 + t_M \approx t_M$ . The seal time,  $t_c + t_w$ , was 10 s in all the tests.

Strength of PC to PEI welds

Strength and ductility (strain to failure) data for PC to PEI hot-tool welds are listed in Table 1. The first two columns give the two hot-tool surface temperatures, the third column gives the heating time  $t_H$ , and the fourth and sixth columns give the weld strength  $\sigma_w$  and the strain at failure  $\epsilon_0$ , respectively. The fifth column gives the strength of the weld relative to that of PC ( $\sigma_{PC} = 67.9$  MPa), the weaker of the two materials. While some data have been obtained for

heating times of  $t_H = 10$  and 20 s, the bulk of the data are for heating times of  $t_H = 15$  s. The hot-tool temperatures were varied from 246–343°C for PC and from 371–427°C for PEI, in steps of 14°C. Figure 3 shows the variations of the relative weld strength  $\sigma_w/\sigma_{PC}$  versus the PC hot-tool temperature for a heating time of 15 s, with the PEI hot-tool temperature as parameter. High relative strengths are obtained for hot-tool temperatures in the range of 302–329°C for PC and 371–399°C for PEI—in which relative strengths on the order of 0.83 can be attained. This is lower than 0.95, the relative strength that has been demonstrated in vibration welds<sup>23</sup>. For the temperature range considered, note that the weld strength (Table 1) for heating times of 10 and 20 s are substantially lower than those for a heating time of 15 s. Because the hot-tool temperature ranges for PC and PEI do not overlap, high weld strengths can only be attained by using dual platen machines.

The seventh column in Table 1 gives the measured change in length,  $\Delta l = l_1 + l_2 - l_0$ , of the specimens caused

Table 1 Strength and ductility data for hot-tool welds of 5.8 mm thick PC to 6.35 mm thick PEI at a strain rate of  $\dot{\epsilon} = 0.01$  s<sup>-1</sup>

Hot-Tool temperature °C		Heating time $t_M$ (s)	Weld strength $\sigma_w$ (MPa)	Relative weld strength $\sigma_w/\sigma_{PC}$	Strain at failure $\epsilon_0$ (%)	$\Delta l$ (mm)	$2\delta_H - \Delta l$ (10 <sup>-2</sup> mm)	Estimates for $\delta_0$ (10 <sup>-2</sup> mm)	
PC	PEI							PC	PEI
274	399	10	31.0	0.46	1.20	1.14	3	1	-13
288	399	10	32.2	0.47	1.16	1.12	0	0	-10
302	399	10	28.4	0.42	1.10	1.22	-10	3	-8
274	427	10	28.3	0.42	1.07	1.46	-34	5	13
288	427	10	34.0	0.50	1.23	1.12	0	0	-14
302	427	10	32.4	0.48	1.26	1.12	0	-3	-11
246	371	15	30.8	0.45	1.06	1.13	-1	4	-10
260	371	15	24.4	0.36	0.92	1.46	-34	4	-13
274	371	15	32.1	0.47	1.13	1.13	-1	0	-13
288	371	15	43.2	0.64	1.55	1.24	-13	0	-15
302	371	15	46.3	0.68	1.92	—	—	9	-13
316	371	15	56.4	0.83	2.35	1.55	-43	9	-10
329	371	15	46.5	0.68	1.86	1.32	-20	5	-11
343	371	15	29.5	0.43	1.07	1.23	-11	1	-19
274	399	15	38.4	0.57	1.68	1.45	-33	0	9
288	399	15	39.5	0.58	1.54	1.50	-38	4	13
302	399	15	55.2	0.81	2.28	1.51	-39	6	8
316	399	15	50.4	0.74	2.07	1.23	-11	4	-15
329	399	15	56.9	0.84	2.54	1.22	-10	3	-18
343	399	15	27.1	0.40	1.03	1.35	-23	4	-10
246	427	15	23.6	0.35	0.81	1.16	-4	6	-20
260	427	15	30.8	0.45	1.14	—	—	8	-10
274	427	15	44.2	0.65	1.63	1.33	-22	6	-11
288	427	15	34.5	0.51	1.22	1.22	-10	-1	-13
288	427	15	54.8	0.81	2.24	1.51	-16	6	8
288	427	15	56.5	0.83	2.44	1.22	-10	3	-18
302	427	15	41.0	0.60	1.86	1.37	-25	4	-11
302	427	15	43.1	0.63	1.69	1.23	-11	5	-24
316	427	15	27.6	0.41	1.08	1.32	-20	4	-13
316	427	15	37.4	0.55	1.43	1.17	-5	-1	-22
329	427	15	48.7	0.72	2.09	1.24	-13	4	-17
329	427	15	27.2	0.40	1.02	1.19	-8	3	-22
343	427	15	18.6	0.27	0.68	1.31	-19	10	-20
246	371	20	27.9	0.41	0.94	1.10	1	0	-5

by material outflow during the welding process. The eighth column gives the differential penetration  $2\delta_H - \Delta l$  that, when thermal expansion effects are ignored, is a measure of whether the stops do ( $\Delta\eta = 0$ ) or do not ( $\Delta\eta > 0$ ) come into contact during the joining phase. Negative values in this column can result from thermal expansion effects contributing to a larger  $\Delta l$  and from errors in the settings for  $\delta_H$  (the actual  $\delta_H$  being larger than that measured). A relatively small combination of measurement errors and thermal expansion of about 0.4 mm could change the sign of  $\Delta\eta$  and explain this apparent inconsistency. In view of the observed negative values of  $\Delta\eta$ , the differential penetration should not be used to infer the status of stops contacting until the issue of negative  $\Delta\eta$  has been resolved.

The ninth and tenth columns give estimates for the settings of  $\delta_0$  for PC and PEI, respectively. As mentioned earlier, fixed micrometer settings were used such that a 76.2 mm long specimen would have melt penetrations of  $\delta_0 = 0.13$  mm. The variations in the estimates for  $\delta_0$  for PC are caused by differences in the lengths of the specimens. The predominantly negative values of  $\delta_0$  for PEI most likely result from incorrect micrometer settings—again, the variations result from differences in the specimen lengths. These negative values of  $\delta_0$  for PEI—indicating lack of surface contact—imply initial surface heating through radiation and conduction through air. Subsequent thermal expansion would quickly result in surface contact with the hot-tool. However, this process would result in a larger effective  $t_0$ .

Note that the relative strengths at a PEI hot-tool temperature of 427°C appear to vary erratically. One reason for this could be variations in the lengths of the PEI and PC specimens causing variations in  $\delta_0$  that affect  $t_M$ . Other possible reasons could be degradation of PEI at this high temperature and deposits on the hot-tool surfaces affecting the cleanliness of the molten plastic layers, and stress concentration effects resulting from a mismatch in the thickness of the specimens for the two materials.

*Strength of PC to PBT welds*

Strength and ductility data for PC and PBT hot-tool welds are listed in Table 2. The relative strengths in the fifth column have been obtained by dividing the weld strength by the strength of PBT ( $\sigma_{PBT} = 65.2$  MPa), the weaker of the two materials. The data are for two heating times of 15 and 20 s. The hot-tool temperatures were varied from 232–316°C for PC and from 246–316°C for PBT. The variations of the relative weld strength  $\sigma_w/\sigma_{PBT}$  versus the PC hot-tool temperature, with the PBT temperature as parameter, are shown in Figure 4 for the two heating times. Very high weld strengths equal to the strength of PBT—the weaker of the two materials—can be attained. These data show that the optimum weld strength not only depends on the hot-tool temperatures, but also on the heating time. For the conditions listed in Table 2, very high relative weld strengths of about unity were attained for hot-tool temperatures in the range 246–260°C for PC and 288–302°C for PBT at the longer heating time of 20 s. These very high weld strengths are consistent with those obtained in vibration welds of these two materials<sup>24</sup>. At the shorter heating time of 15 s, relative weld strengths of about 0.9 can be attained for hot-tool temperature combinations of 274°C for PC and 302°C for PBT, and 288°C for PC and 274°C for PBT. These sparse data, in which tests were not repeated at each process condition to assess repeatability, would seem to indicate that the use of the same hot-tool temperature in

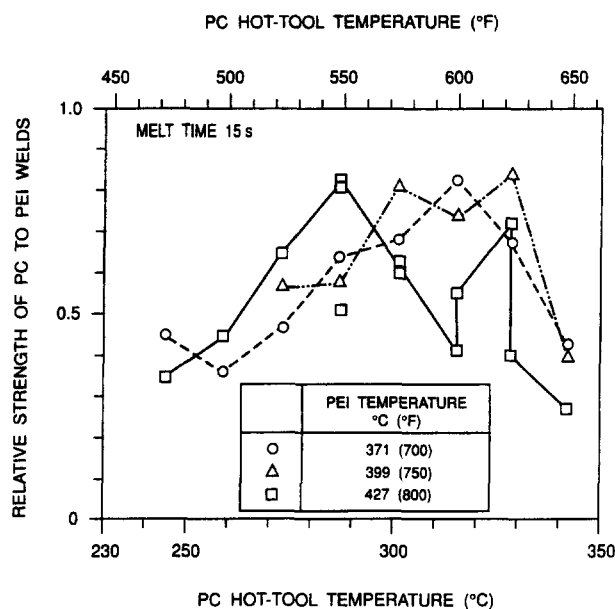


Figure 3 Variation of the relative strength of PC to PEI hot-tool welds versus the PC hot-tool temperature, with the PEI hot-tool temperature as parameter, for a heating time of 15 s

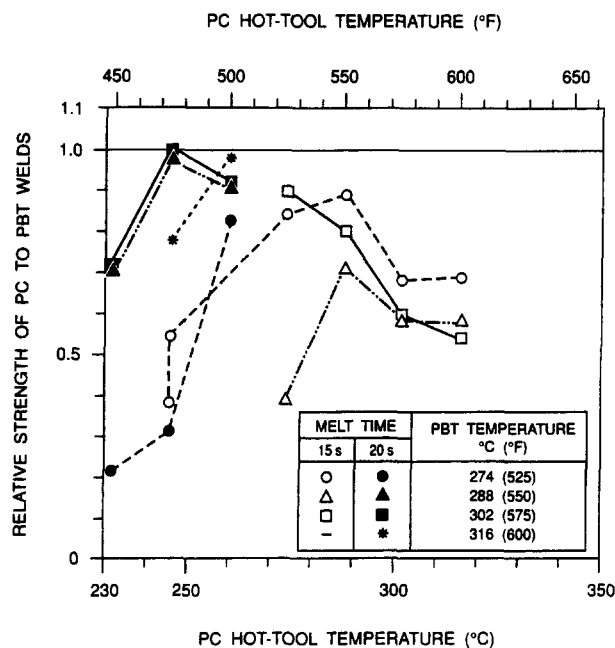


Figure 4 Variation of the relative strength of PC to PBT hot-tool welds versus the PC hot-tool temperature, with the PBT hot-tool temperature as parameter, for heating times of 15 and 20 s

the range 274–288°C can give relative weld strengths of about 0.85. By optimizing other parameters, such as the melt penetration  $\delta_H$  and the melt time  $t_M$ , it may be possible to establish a hot-tool temperature process window over which very high weld strengths can be attained by using the same temperature for both the materials. The optimum  $\delta_H$  and  $t_M$  may depend on the temperature used. The availability of such a process window would make it possible to attain high weld strengths on the more conventional single platen machines.

As in the case of PC to PEI welds (Table 1), the eighth column in Table 2 also shows negative values of  $\Delta\eta$ —although the magnitudes of these negative numbers are somewhat smaller. Also, as in Table 1, the tenth column in

**Table 2** Strength and ductility data for hot-tool welds of 5.8 mm thick PC to 6.35 mm thick PBT at a strain rate of  $\dot{\epsilon} = 0.01 \text{ s}^{-1}$

Hot-Tool Temperature °C		Heating time $t_H$ (s)	Weld strength $\sigma_w$ (MPa)	Relative weld strength $\sigma_w/\sigma_{PBT}$	Strain at failure $\epsilon_0$ (%)	$\Delta l$ (mm)	$2\delta_H - \Delta l$ ( $10^{-2}$ mm)	Estimates for $\delta_0$ ( $10^{-2}$ mm)	
PBT	PC							PBT	PC
246	302	15	32.8	0.50	1.31	1.17	-5	4	-14
260	302	15	25.4	0.39	0.97	1.17	-5	4	-17
274	246	15	36.0	0.55	1.32	0.99	13	-4	-14
274	246	15	25.7	0.39	0.99	0.90	22	8	-18
274	274	15	55.4	0.85	2.31	1.10	1	5	-20
274	288	15	58.7	0.90	2.73	1.14	-3	0	-19
274	302	15	44.8	0.69	1.88	1.30	-18	3	-14
274	316	15	45.6	0.70	1.88	1.36	-24	-4	-4
288	274	15	25.9	0.40	1.10	—	—	6	-14
288	288	15	47.1	0.72	1.99	—	—	6	-15
288	302	15	39.1	0.60	1.60	—	—	3	-15
288	316	15	38.4	0.59	1.56	—	—	4	-15
302	274	15	59.1	0.91	2.78	—	—	4	-1
302	288	15	52.7	0.81	2.16	—	—	9	-1
302	302	15	38.9	0.60	1.53	—	—	0	-9
302	316	15	35.7	0.55	1.53	—	—	5	-18
274	232	20	14.5	0.22	0.51	0.69	43	0	-17
288	232	20	46.1	0.71	1.93	0.91	20	1	-17
302	232	20	47.3	0.73	2.15	1.16	-4	1	-9
274	246	20	20.6	0.32	0.71	1.01	10	0	-19
288	246	20	64.2	0.98	4.09	1.22	-10	5	-18
302	246	20	65.3	1.00	4.96	1.26	-1	-1	-15
316	246	20	51.2	0.79	2.33	1.27	-15	-3	-15
274	260	20	54.5	0.84	2.51	1.10	1	0	-15
288	260	20	60.2	0.92	3.12	1.22	-10	4	-14
302	260	20	60.5	0.93	3.08	1.18	-6	3	-14
316	260	20	64.5	0.99	3.86	1.24	-13	1	-17

**Table 3** Strength and ductility data for hot-tool welds of 6.35 mm thick PEI to PBT at a strain rate of  $\dot{\epsilon} = 0.01 \text{ s}^{-1}$

Hot-Tool Temperature °C		Heating time $t_H$ (s)	Weld strength $\sigma_w$ (MPa)	Relative weld strength $\sigma_w/\sigma_{PBT}$	Strain at failure $\epsilon_0$ (%)	$\Delta l$ (mm)	$2\delta_H - \Delta l$ ( $10^{-2}$ mm)	Estimates for $\delta_0$ ( $10^{-2}$ mm)	
PBT	PEI							PBT	PEI
274	371	15	27.5	0.42	0.92	0.99	13	4	-14
274	427	15	21.5	0.33	0.65	1.33	-22	1	-13
274	371	20	31.3	0.48	1.11	1.16	-4	6	-18
274	371	20	30.9	0.47	1.01	1.10	1	3	-13
274	371	20	30.8	0.47	1.10	—	—	-6	-15
288	371	20	26.4	0.41	0.80	1.14	-3	-4	-11
288	371	20	36.7	0.56	1.41	—	—	1	-14
302	371	20	36.2	0.55	1.15	1.22	-10	4	-11
302	371	20	30.9	0.47	1.13	—	—	4	-10
260	399	20	35.0	0.54	1.26	1.31	-19	11	-17
274	399	20	42.0	0.64	1.49	—	—	3	-10
288	399	20	37.8	0.58	1.41	—	—	0	-11
302	399	20	28.2	0.43	0.97	—	—	0	-15
260	427	20	32.7	0.50	1.16	1.32	-20	3	-19
274	427	20	58.8	0.90	2.84	1.35	-23	8	-18
274	427	20	44.3	0.68	1.63	1.26	-14	1	-18
288	427	20	47.7	0.73	1.76	1.37	-3	5	-13
302	427	20	44.6	0.68	1.73	1.33	-22	3	-17

Table 2 shows negative values of  $\delta_0$ , which (refer to discussion on PC to PEI welds) would result in an increased 'effective'  $t_0$ .

*Strength of PEI to PBT welds*

Strength and ductility data for PEI to PBT hot-tool welds are listed in Table 3. While some data are reported for a heating time of 15 s, the bulk of the data are for  $t_H = 20$  s. The relative strengths in the fifth column are based on a PBT strength of 65.2 MPa. The hot-tool temperatures were varied from 260–303°C for PBT and from 371–427°C for PEI. Figure 5 shows the variations of the relative weld strength versus the PBT hot-tool temperature for a heating time of 20 s, with the PEI hot-tool temperature a parameter. These rather sparse data seem to indicate that relative weld strengths of about 0.9 can be attained at hot-tool temperatures of 274°C for PBT and 427°C for PEI. This is lower than 0.95, the relative strength that has been demonstrated in PBT to PEI vibration welds (unpublished data). The two data points (Table 3) for a heating time of 15 s indicate much lower strengths. At the hot-tool temperature of 427°C for PEI, relative weld strengths in the range of 0.68–0.73 can be attained for PBT hot-tool temperatures in the range 274–302°C. Because the hot-tool temperature ranges for PEI to PBT welds do not overlap, high weld strengths can only be obtained by using a dual platen machine—as in the case of PC to PEI welds.

Here again, as in PC to PEI and PBT to PC welds, the eighth column (Table 3) shows negative values of  $\Delta\eta$ . And, as in the previous two tables, the last column shows negative melt penetrations.

CONCLUDING REMARKS

High strengths have been demonstrated in hot-tool welds between very dissimilar materials. For example, although the two immiscible, amorphous polymers PC and PEI have glass transition temperatures of 150°C and 215°C, respectively, weld strengths comparable to the strength of PC can be attained. In hot-tool welds of PC to the

semicrystalline polymer PBT ( $T_M = 225^\circ\text{C}$ ,  $T_g = 60^\circ\text{C}$ ) weld strengths equal to that of PBT are attainable. In welds of PBT to PEI, relative weld strengths of about 0.9 have been attained.

High strengths in PC to PEI welds can only be attained over nonoverlapping hot-tool temperature ranges for the corresponding hot-tool surfaces for the two materials. This is also true for PBT to PEI welds. Thus, the use of different hot-tool temperatures for each of the two materials being welded is important for obtaining high strengths in welds between dissimilar materials. In some dissimilar material pairs, such as PC and PBT, it may be possible to attain high weld strengths by using the same hot-tool temperatures for both the materials. In such cases, a single platen machine would be adequate. While the hot-tool temperatures used are likely to be the most important process variables, the weld strength also depends on the heating time.

The hot-tool welding of dissimilar thermoplastics involves many process variables. For example, the hot-tool settings  $\delta_H$  and the initial penetration  $\delta_0$  could be different for the two sides. In this paper, the same stop settings have been used for the two sides. In addition, all the data have been obtained at one stop setting. While the sparse data presented in this paper have shown that dissimilar materials can be hot-tool welded, optimum process conditions have not necessarily been established. In particular, the effects of  $\delta_0$  and  $\delta_H$  have not been evaluated—even for the case of the same stop setting on both sides. Also, combinations of hot-tool temperatures and heating times have not been adequately explored.

The eighth columns in Tables 1–3 show negative values of  $\Delta\eta$ , which could result from thermal expansion effects that have not been accounted for. However, this apparent discrepancy should not be a concern because it may be an artifact of the way  $\Delta\eta$  has been defined. On the other hand, the negative values of  $\delta_0$  in the eighth columns may be an indication of incorrect micrometer settings on the right-hand specimen holder. While these negative melt penetrations may change how the right-hand hot-tool surface temperature affects welding, and may be equivalent to an apparent increase in  $t_0$ , they do not affect the conclusions relating to the relative strengths that can be achieved in welds of the three dissimilar resins considered.

ACKNOWLEDGEMENTS

This work was supported by GE Plastics. The contributions of K. R. Conway, who carried out all the tests, and the inputs of L. P. Inzinna are greatly appreciated.

REFERENCES

1. Stokes, V. K., *Polym. Eng. Sci.*, 1989, **29**, 1310.
2. Potente, H. and Natrop, J., *Polym. Eng. Sci.*, 1989, **29**, 1649.
3. Barber, P. and Atkinson, J. R., *J. Mater. Sci.*, 1972, **7**, 1131.
4. Barber, P. and Atkinson, J. R., *J. Mater. Sci.*, 1974, **9**, 1456.
5. Bucknall, C. B., Drinkwater, I. C. and Smith, G. R., *Polym. Eng. Sci.*, 1980, **20**, 432.
6. Egen, U. and Ehrenstein, G. W., *DVS Berichte*, 1983, **84**, 49.
7. Andrews, J. R. F. and Bevis, M., *J. Mater. Sci.*, 1984, **19**, 645.
8. Andrews, J. R. F. and Bevis, M., *J. Mater. Sci.*, 1984, **19**, 653.
9. Watson, M. N. and Murch, M. G., *Polym. Eng. Sci.*, 1989, **29**, 1382.
10. Gehde, M., Bevan, L. and Ehrenstein, G. W., *Polym. Eng. Sci.*, 1992, **32**, 586.
11. Bowman, J., Haunton, J. and Folkes, M. J., *SPE ANTEC Tech. Papers*, 1990, **36**, 1793.

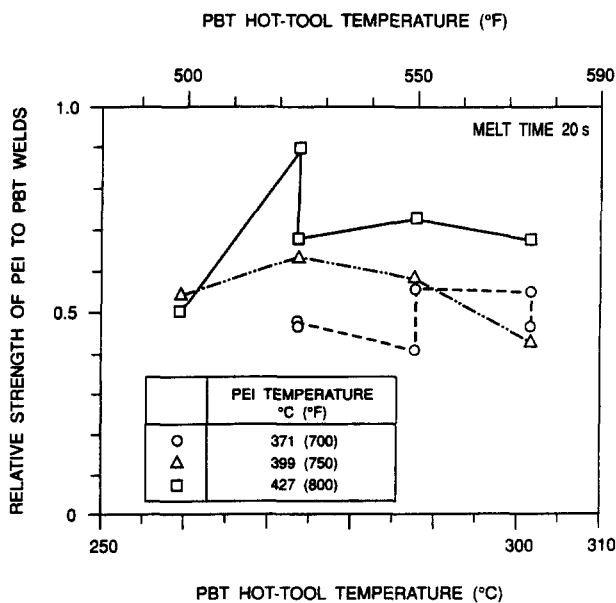


Figure 5 Variation of the relative strength of PEI to PBT hot-tool welds versus the PBT hot-tool temperature, with the PEI hot-tool temperature as parameter, for a heating time of 20 s



*Experiments on the hot-tool welding of three dissimilar thermoplastics: Vijay K. Stokes*

12. Potente, H., *Kunststoff*, 1977, **67**, 17.
13. Potente, H., *DVS Berichte*, 1983, **84**, 41.
14. Potente, H. and Tappe, P., *Polym. Eng. Sci.*, 1989, **29**, 1642.
15. Pimputkar, S. M., *Polym. Eng. Sci.*, 1989, **29**, 1387.
16. Poslinski, A. J. and Stokes, V. K., *Polym. Eng. Sci.*, 1992, **32**, 1147.
17. Poslinski, A. J. and Stokes, V. K., *SPE ANTEC Tech. Papers*, 1992, **38**, 1228.
18. Gabler, K. and Potente, H., *J. Adhesion*, 1980, **11**, 145.
19. Potente, H. and Gabler, H., *Plastverarbeiter*, 1980, **31**, 203.
20. El Barbari, N., Michel, J. and Menges, G., *Kunststoffe*, 1986, **76**, 20.
21. El Barbari, N., Michel, J. and Menges, G., *Kunststoffberater*, 1986, **31**, 63.
22. Muschik, H., Radax, M., Dragaun, H. and Eichinger, F., *Kunststoffe*, 1986, **76**, 23.
23. Stokes, V. K. and Hobbs, S. Y., *Polym. Eng. Sci.*, 1989, **29**, 1667.
24. Hobbs, S. Y. and Stokes, V. K., *Polym. Eng. Sci.*, 1991, **31**, 502.
25. Stokes, V. K. and Hobbs, S. Y., *Polymer*, 1993, **30**, 1222.
26. Stokes, V. K., *Polym. Eng. Sci.*, 1997, **37**, 692.